Propagation Characteristics of Superconducting Microstrip Lines

Shau-Gang Mao, Jeng-Yi Ke, and Chun Hsiung Chen

Abstract— **The modified spectral-domain approach is applied to study the propagation characteristics of high temperature superconducting microstrip lines whose signal strip and ground plane are of arbitrary thickness. In this study, numerical results for effective dielectric constant, attenuation constant, and strip current distribution are presented to discuss the effects due to frequency, temperature, strip thickness, and substrate loss tangent. In particular, the conductor and dielectric attenuation constants of superconducting microstrip line are depicted separately to discuss the mechanism of the line losses. A comparison with published theoretical and experimental results is also included to check the accuracy of the new approach's results.**

I. Introduction

HIGH-TEMPERATURE superconductors (HTS) are characterized by low surface resistance and frequency-independent penetration depth. These properties make them attractive in the development of some special microwave devices. As a result of low surface resistance and hence low loss, the implementation of high-Q resonators [1], [2], long delay lines [3]–[5], and low-loss filters [6], [7] with a sharp frequency response becomes possible. The frequency-independent nature of penetration depth also leads to lower distortion in a HTS transmission line [8]. The above merits and slow wave characteristics associated with the HTS thin-film technology make it possible to manufacture a compact-size circuit in microwave systems.

The HTS microstrip lines have been characterized by using the simplified quasi-TEM approaches. In [9], the phenomenological loss equivalence method was proposed to analyze the line whose strip thickness was in the order of the penetration depth. The slow wave propagation characteristic along a superconducting microstrip line was investigated by the spectral-domain technique [10] in which the superconducting strip was modeled by an equivalent surface impedance when the strip was either much thinner or much thicker than the penetration depth. By treating the superconducting strip as a system of coupled strip lines, Sheen *et al.* [11] have utilized the quasi-TEM approach to find the current distribution, resistance, and inductance matrices. However, the above-mentioned methods have the assumption of small longitudinal field components and are not applicable in the higher frequency regime.

Several full-wave analyses have recently been proposed to deal with the HTS transmission lines [12]–[19]. The techniques of finite-difference [12] and mode-matching [13] were applied to investigate the microstrip lines and coplanar waveguides, but they can only handle the bounded structures. In [14] and [15], the spectral-domain immittance approach (SDIA) together with the complex boundary condition was proposed to analyze the microstrip structure with isotropic or anisotropic substrates. This SDIA is limited to the structures whose strip thickness, in comparison with the penetration depth, is very thin or very thick. By representing the lossy strip by an equivalent impedance surface, Van Deventer *et al.* [16] have used an integral equation approach to treat the shielded HTS microstrip line; however, this surface was characterized by a frequency-dependent impedance which was derived from a quasi-TEM analysis of the fields and currents inside the superconducting strip. A space domain boundary integral equation method [17] was applied for a full-wave loss analysis of coplanar stripline and microstrip line configurations with Au and YBCO strips. Lee *et al.* [18], [19] further employed the spectral-domain volume integral equation to analyze the superconducting microstrip lines with perfectly conducting ground planes. In [18], an integral equation formulation was proposed for an anisotropic superconducting strip and then solved by the Galerkin's method with rooftop basis functions. In [19], single and coupled superconducting microstrip lines on anisotropic substrates were investigated by the equivalent surface impedance approach.

In this study, the newly proposed modified spectral-domain approach [20] is applied to analyze the superconducting microstrip line with arbitrary thickness in signal strip and ground plane. Here, all three components of strip current with two-dimensional dependence are included and the lossy effects of both superconductors and substrates are investigated in detail. To improve the computational efficiency, suitable basis functions such as piecewise linear and penetration-depth dependent exponential bases are chosen for the unknown strip current so that the integral equation may be simplified by analytically integrating it along one coordinate variable. To provide more information for superconducting microstrip lines, some interesting results such as a comparison of propagation characteristics for superconductor, normal conductor, and perfectly electric conductor lines and a separate discussion of conductor and substrate losses are also included.

Manuscript received October 6, 1994; revised October 2, 1995. This work was supported by the National Science Council of Taiwan, Republic of China, Grant NSC 83-0404-E-002-044.

The authors are with the Department of Electrical Engineering, National Taiwan University, Taipei, Taiwan 10617, Republic of China.

Publisher Item Identifier: S 0018-9480(96)00466-8.

II. Formulation

The superconducting microstrip line (Fig. 1(a)) under consideration consists of a signal strip of width w, thickness t, and a ground plane of thickness b. Both signal strip and ground plane are made of superconductor of complex conductivity σ. This line has a substrate whose dielectric constant and loss tangent are ϵ_r and $\tan\delta$, respectively. With the field dependence $e^{j(\omega t - k_z z)}$ assumed throughout the analysis, the superconductor may be characterized by the two-fluid conductivity model [21]

$$\sigma = \sigma_n \left(\frac{T}{T_c}\right)^4 - j\frac{1}{\omega\mu_0\lambda^2}, \qquad T \le T_c. \tag{1}$$

Here σ_n is the normal state conductivity at critical temperature T_c

$$\lambda = \frac{\lambda_0}{\sqrt{1-\left(\frac{T}{T_c}\right)^4}} \tag{2}$$

is the penetration depth at temperature T, and λ_0 is the one at 0 K. Although the high-T_c superconductor is considered anisotropic, the effect of this anisotropy may be neglected in the characterization of a microstrip transmission line [18].

To solve this problem by the modified spectral-domain approach [20], the equivalent structure shown in Fig. 1(b) is investigated. In this equivalent problem, the signal strip region Ω is replaced by the free space and the equivalent current $\mathbf{J}(\mathbf{r}) = \sigma\mathbf{E}(\mathbf{r})$. Then the relationship between the electric field $\mathbf{E}(\mathbf{r})$ and the current density $\mathbf{J}(\mathbf{r}')$ in the region Ω may be written as

$$\mathbf{E}(\mathbf{r}) = \int_\Omega \bar{\bar{\mathbf{G}}}(\mathbf{r}-\mathbf{r}') \bullet \mathbf{J}(\mathbf{r}')\,d\mathbf{r}' = \frac{1}{\sigma}\mathbf{J}(\mathbf{r}). \tag{3}$$

Here, $\bar{\bar{\mathbf{G}}}$ is the dyadic Green's function for the multilayer structure as shown in Fig. 1(c). It should be emphasized that the superconducting ground plane is now regarded as a lossy layer of parameters σ and b therefore the effect of this lossy ground plane may be discussed by this Green's function. Some detail of the Green's function is presented in the Appendix.

By weighting both sides of (3) by an arbitrary function $\mathbf{w}(\mathbf{r})$ and then integrated over Ω, one may get a homogeneous integral equation for the unknown strip current $\mathbf{J}(\mathbf{r})$

$$\int_{\frac{-w}{2}}^{\frac{w}{2}}\int_0^t \mathbf{w}(x,y) \bullet \left[\int_{\frac{-w}{2}}^{\frac{w}{2}}\int_0^t \bar{\bar{\mathbf{G}}}(x,y,x',y',k_z) \bullet \mathbf{J}(x',y')\,dy'\,dx' - \frac{\mathbf{J}(x,y)}{\sigma}\right] dy\,dx = 0. \tag{4}$$

With the parameters (b,σ) of superconducting ground plane absorbed in the Green's function, the only unknowns are the current distributions within the signal strip which can be expressed as

$$\mathbf{J}_i(x,y) = \sum_{j=0}^{m}\sum_{k=0}^{n} c_i^{jk}\psi_i^j(x)\phi_i^k(y), \qquad i = x,y,z. \tag{5}$$

Here $(m+1)$ x-dependent and $(n+1)$ y-dependent bases are included in the approximation of the strip current. It should be pointed out that to get a more accurate result, all three components of strip current should be included in the analysis.

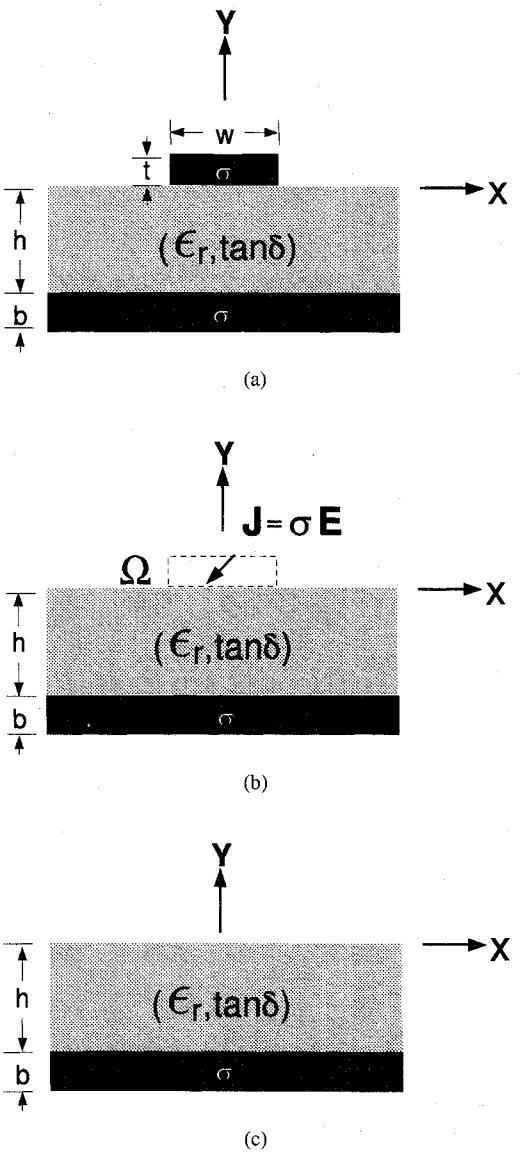

Fig. 1. (a) Cross section of superconducting microstrip line, (b) equivalent problem in formulation, and (c) layer structure for deriving Green's function.

In this study, the Legendre polynomials are chosen as the x-dependent bases for the unknown strip current $\mathbf{J}$

$$\psi_z^l(x) = \psi_y^l(x) = P_{2l}\left(\frac{x}{w/2}\right),$$
$$\psi_x^l(x) = P_{2l+1}\left(\frac{x}{w/2}\right). \tag{6}$$

For simplicity, the following piecewise linear functions are chosen as the y-dependent bases for $\mathbf{J}$

$$\phi_z^l(y) = \phi_x^l(y) = \phi_y^l(y) = \wedge(y) = \begin{cases} \frac{y-\triangle_{l-1}}{\triangle}, & \triangle_{l-1} < y < \triangle_l \\ \frac{\triangle_{l+1}-y}{\triangle}, & \triangle_l < y < \triangle_{l+1} \\ 0, & \text{otherwise} \end{cases} \tag{7}$$

where $\triangle_l = l\triangle$ and $\triangle = t/n$. To better represent the exponential-decay behavior of strip current inside the su-

perconductor, we alternatively use the following exponential functions for the y-dependent bases, especially in the higher frequency regime

$$\phi_z^l(y) = \phi_y^l(y) = \phi_x^l(y) = \begin{cases} \exp[-(\frac{1}{\lambda} + j\frac{\lambda}{\delta^2})ly], & l \geq 0 \\ \exp[-(\frac{1}{\lambda} + j\frac{\lambda}{\delta^2})l(y-t)], & l < 0. \end{cases} \quad (8)$$

Here $\delta = \sqrt{\frac{2}{\omega\mu_0\sigma_n}}$ is the conventional skin depth, and the terms $l \geq 0$ and $l < 0$ describe the current distributions over the lower and upper sides of signal strip, respectively.

By applying the Fourier transformation

$$\tilde{A}(k_x) = \int_{-\infty}^{\infty} A(x)e^{-jk_x x}\,dx$$
$$A(x) = \frac{1}{2\pi}\int_{-\infty}^{\infty} \tilde{A}(k_x)e^{jk_x x}\,dk_x \quad (9)$$

and Parseval's theorem with respect to x variable to (4), then analytically integrating it with respect to y variable, one may finally yield the governing equation in the spectral domain

$$\int_{-\infty}^{\infty} \tilde{w}(k_x)[\tilde{Z}(k_x, k_z) - \tilde{P}(k_x)]\tilde{J}(k_x)\,dk_x = 0. \quad (10)$$

Note that the y-dependence form of the spectral-domain Green's function $\tilde{G}$ is a linear combination of $\exp(j\beta_0 y)$ and $\exp(j\beta_0 y')$, where β_0 is independent of y or y' (see Appendix). By a proper choice of the y-dependent bases such as (7) or (8), the y-dependent integration in (4) may be analytically integrated and this implies that only single integration with respect to k_x is involved in the final spectral-domain (10). Thus, it can use the conventional technique of spectral-domain approach to find the phase constant β and attenuation constant α.

To derive the matrix equation for the propagation constant from the spectral-domain (10), the Galerkin's method is used, in which the bases for $\mathbf{w}(x, y)$ are the same as those for $\mathbf{J}(x, y)$. Then the propagation constant $k_z = \beta - j\alpha$ can be found by solving this homogeneous matrix equation.

III. Numerical Results

Numerical results such as effective dielectric constant $\epsilon_{\text{eff}} = (\beta/k_0)^2 (k_0^2 = \omega^2\mu_0\epsilon_0)$, attenuation constant α, and longitudinal current distributions J_z over signal strip are investigated in detail.

Regarding the convergence behavior with respect to the expansion in (5) and the proper choice of the y-dependent bases in (7) and (8), one should notice the following thickness criterion on the signal strip. If the signal strip thickness t is greater than three times of the penetration depth λ, the number $(n+1)$ of the y-dependent piecewise linear bases will be greater than that of the exponential bases, both to give same accuracy. Because the CPU time is directly proportional to the square of the number of the y-dependent bases, the use of exponential bases is essential in reducing the computing time in higher frequency. To get convergent results for ϵ_{eff} and α, we use seven Legendre polynomials for the x-dependent bases; but we use seven piecewise linear y-dependent bases when $t < 3\lambda$ and three exponential y-dependent bases when $t > 3\lambda$.

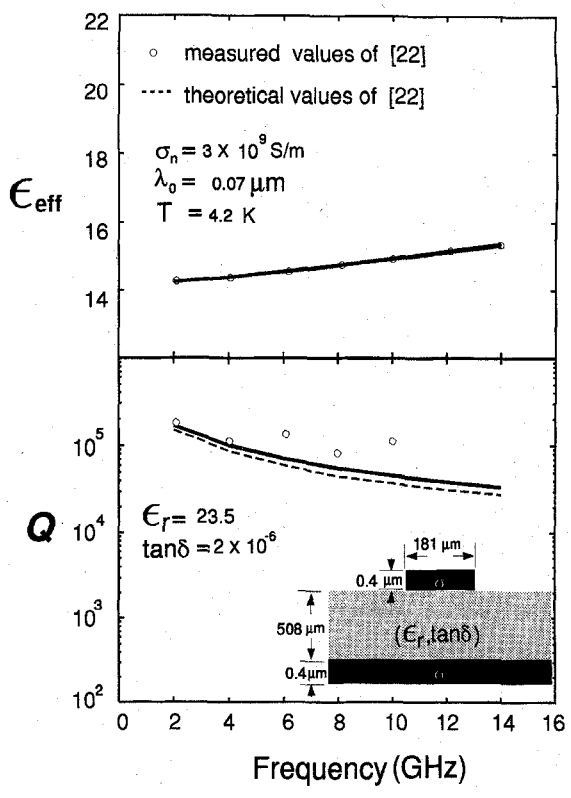

Fig. 2. Comparison of effective dielectric constant ϵ_{eff} and quality factor Q with those of [22].

The effective dielectric constant ϵ_{eff} and quality factor $Q(=\beta/2\alpha)$ based on the modified spectral-domain approach (MSDA) are presented in Fig. 2 and are compared with the theoretical and measured ones from the spectral-domain volume integral equation method [22]. Agreement with other works (not shown) and better fitting with measured values of [22] confirm the validity of the proposed MSDA for superconducting microstrip lines.

Comparison among characteristics of superconducting (SC), normal conducting (NC), and perfectly electric conducting (PEC) microstrip lines is shown in Fig. 3. Because the field penetration inside superconductor is independent of frequency as described by the penetration depth λ in (2), both SC and PEC lines show less material dispersion than the NC line for frequency less than 10 GHz. The difference in ϵ_{eff}-curves between SC and NC lines is not negligible when the operating frequecy is lower. In the higher frequency range, all SC, NC, and PEC lines have similar dispersion characteristics because field distributions are now almost identical. Superconducting line is essentially nondispersive in lower frequency range but it will be dispersive like the normal conducting line due to the similar field distributions inside the substrate at higher frequency. By the similarity of ϵ_{eff}-curves for both SC and PEC lines, the superconducting line may easily be analyzed by regarding its conductivity first as infinity to get the effective dielectric constant and the fields, and then use these fields and the power-loss method [23] to approximately calculate the attenuation caused by the superconductors. Fig. 3 also presents

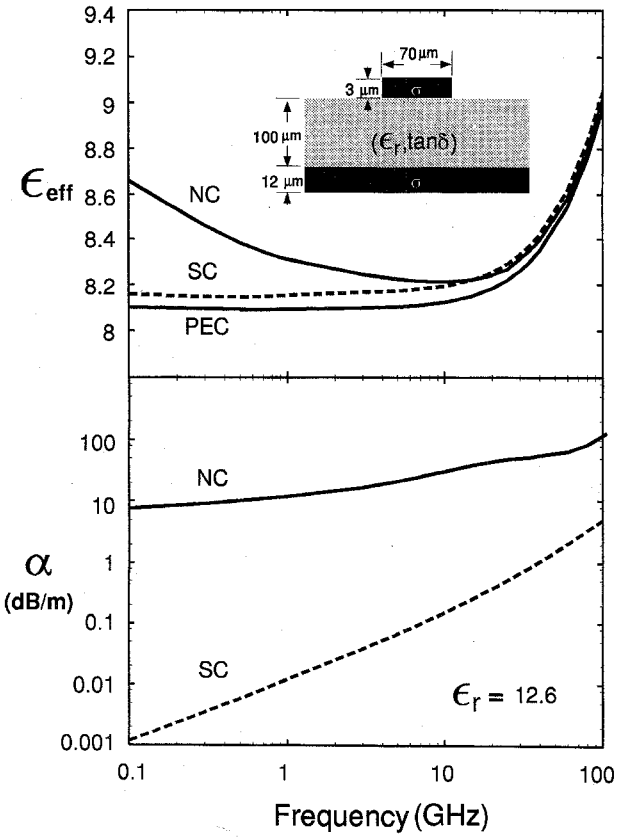

Fig. 3. Effective dielectric constant ϵ_{eff} and attenuation constant α for superconducting (SC), normal conducting (NC), and perfectly electric conducting (PEC) lines. SC(YBCO): $\sigma_n = 7.46 \times 10^6$ (S/m), $\lambda_0 = 0.18$ μm, $\tan\delta = 3\times10^{-5}$, and $T = 77$ K; NC (copper): conductivity $= 5.76\times10^7$ (S/m), $\tan\delta = 3 \times 10^{-4}$, and $T = 300$ K.

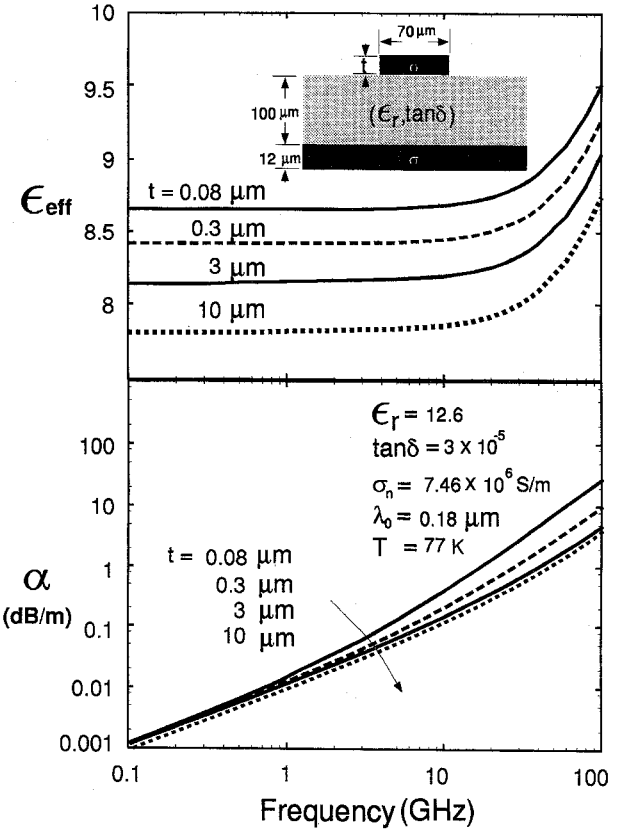

Fig. 4. Effective dielectric constant ϵ_{eff} and attenuation constant α versus frequency with strip thickness t as parameters.

the low loss property of SC line. The nearly straight line behavior in the α-curve helps us to predict the attenuation characteristics at any frequency. For frequency higher than 12 GHz, SC and NC lines have nearly the same effective dielectric constant but the attenuation constant of NC line is almost two orders of magnitude larger than that of SC line.

The dispersion and attenuation properties of superconducting microstrip line for various strip thickness t are depicted in Fig. 4. Both ϵ_{eff} and α decrease as strip thickness t increases; the former is due to the increase of the field distribution inside the air region and the latter due to the decrease of the line kinetic resistance [11].

Fig. 5 shows the effect of temperature on ϵ_{eff} and α with strip thickness t as parameters. Variation in ϵ_{eff} and α is small for the normalized temperature T/T_c ranging from 0.05 to 0.7. The temperature dependence of both ϵ_{eff} and α would be reduced by increasing the strip thickness. Hence, using thicker superconducting strips or lower temperature may reduce the characteristics fluctuation due to temperature variation.

The attenuation due to lossy substrate is important in superconducting lines and will be discussed in Figs. 6–8. The effect of increasing loss tangent $\tan\delta$ is represented in Fig. 6. Note that the changing rate, with respect to frequency, of the attenuation due to conductors only ($\tan\delta = 0$) is larger than that due to both conductors and dielectrics ($\tan\delta = 3\times10^{-3}$, 3×10^{-4}, and 3×10^{-5}).

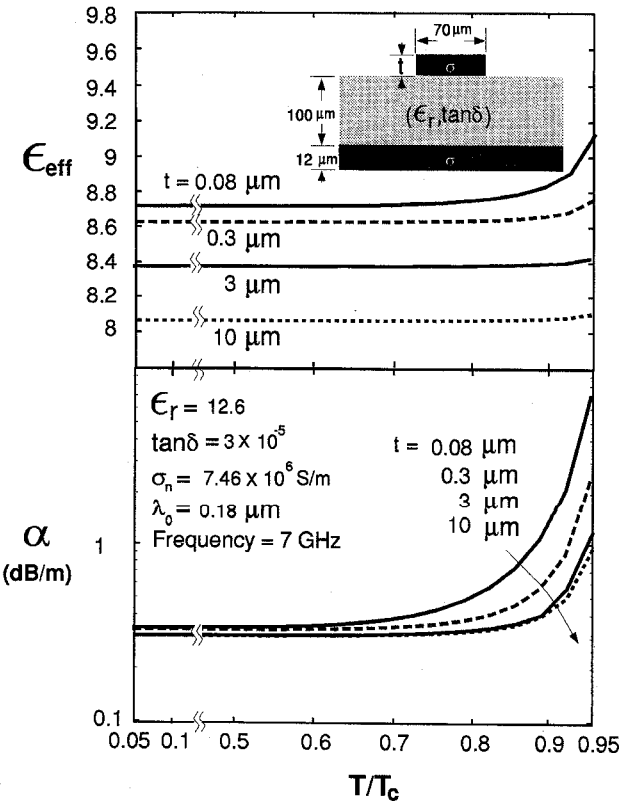

Fig. 5. Effective dielectric constant ϵ_{eff} and attenuation constant α versus normalized temperature T/T_c with strip thickness t as parameters.

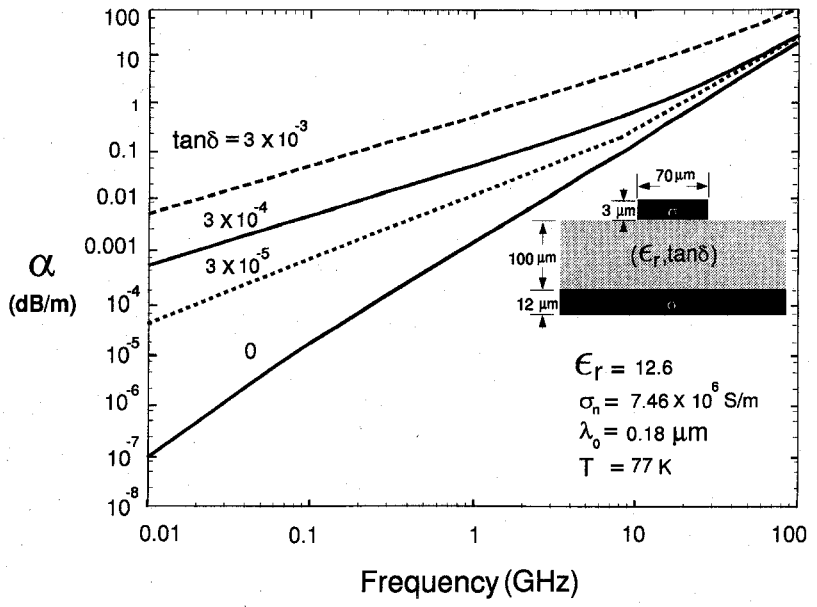

Fig. 6. Attenuation constant α versus frequency with loss tangent $\tan\delta$ of substrate as parameters.

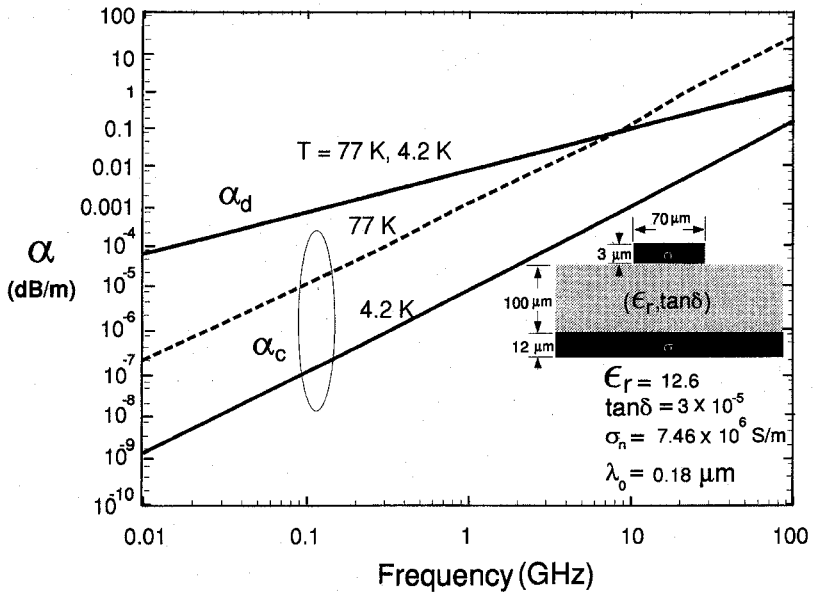

Fig. 7. Conductor attenuation constant α_c and dielectric attenuation constant α_d versus frequency with temperature T as parameters.

Now we separately discuss the attenuations from conductor loss and dielectric loss. The conductor attenuation constant α_c of superconducting line is calculated from the lossless-substrate structure with $\tan\delta = 0$. The dielectric attenuation constant α_d is calculated from the difference between the attenuation α for the lossy-substrate structure with $\tan\delta(= 3 \times 10^{-5})$ and the one α_c for the lossless-substrate structure with $\tan\delta = 0$. Here in evaluating the dielectric attenuation constant α_d, the field distributions of the line with lossless substrate $(\tan\delta = 0)$ are assumed to be identical with those of the same line structure but with lossy substrate $(\tan\delta = 3 \times 10^{-5})$. Fig. 7 shows α_c and α_d versus frequency with operating temperature T as parameters. As frequency increases, the α_c-curve increases more steeply than the α_d-curve such that α_c is larger than α_d for frequency above 8 GHz at 77 K. The α_c- and α_d-curves versus normalized temperature with frequency as parameters are also shown in Fig. 8. The dielectric attenuation constant α_d is independent of temperature but the conductor attenuation constant α_c increases rapidly as temperature increases. As expected, the attenuation constant of superconducting microstrip line is dominated by the dielectric loss except at higher frequency and higher temperature.

The longitudinal current distributions on the signal strip of superconducting (SC) and normal conducting (NC) microstrip lines are shown in Fig. 9. Here in computing the strip current, the piecewise linear functions (7) are adopted as the y-dependent bases. The total current carried by the strip is

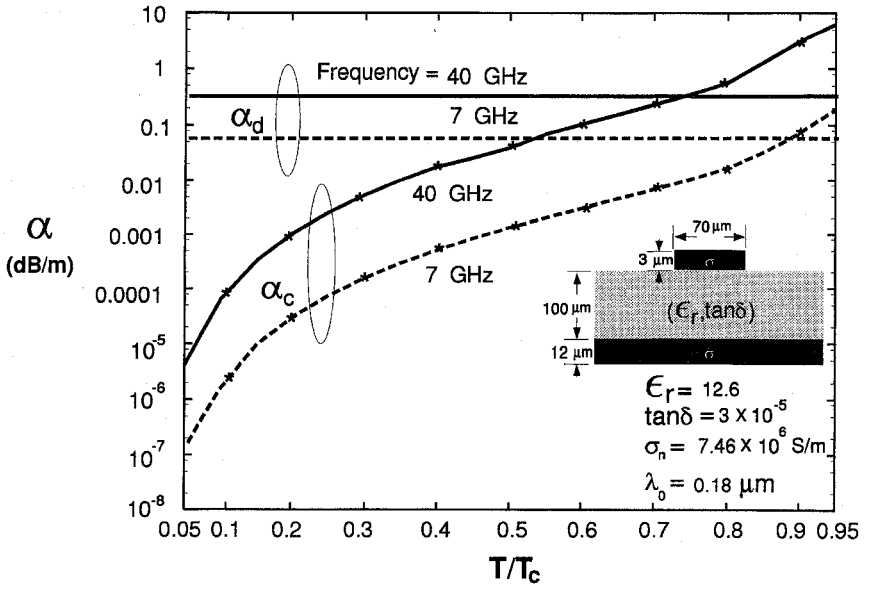

Fig. 8. Conductor attenuation constant α_c and dielectric attenuation constant α_d versus normalized temperature T/T_c with frequency as parameters.

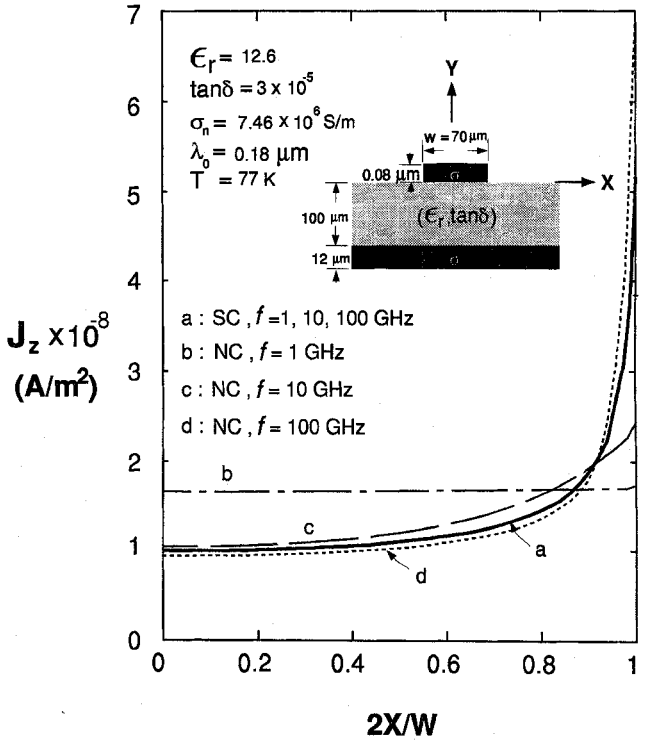

Fig. 9. Longitudinal current distributions on signal strip of superconducting (SC) and normal conducting (NC) lines (at $y = 0$).

assumed to be 30 mA and the superconducting current density must be less than the critical value $J_c (\simeq 10^{10}$ A/m$^2)$ for maintaining the superconducting state. As excepted, the edge enhancement behavior is found for the longitudinal current J_z with respect to x-coordinate, but the edge current is finite instead of infinity [24]. Even using the thinner strip with thickness $t = 0.08$ μm, the maximum superconducting current density at the strip edge is still smaller than J_c. Because λ/t is about 3, the longitudinal current distributes uniformly in the y-direction (not shown). Note that the current distribution over SC strip is independent of frequency from 1 GHz to 100 GHz, however the current distribution over NC strip shows dependence on frequency as expected.

IV. Conclusion

The modified spectral-domain approach has been applied to analyze the superconducting microstrip line with layer structure in which the thickness of signal strip and ground plane are arbitrary. Numerical results such as effective dielectric constant ϵ_{eff}, attenuation constant α (especially the conductor attenuation constant α_c and dielectric attenuation constant α_d), and longitudinal strip current distribution have been presented to discuss the effects on propagation characteristics due to variations in frequency, temperature, strip thickness, and substrate loss tangent etc.

Some observations are worthy of mention. Similar ϵ_{eff}-curves for normal conductor, superconductor, and perfectly electric conductor lines are observed at higher frequency, but the difference in ϵ_{eff}-curves between normal conductor and superconductor lines is not negligible at lower frequency. A separate discussion of the conductor and substrate losses further reveals that the conductor attenuation constant α_c may be greater than the dielectric attenuation constant α_d at higher frequency and higher temperature. The longitudinal current density on the signal strip of superconducting line is found smaller than J_c and its distribution is independent of frequency from 1 GHz to 100 GHz.

The proposed approach can easily be extended to the structures of superconducting coplanar strips and coplanar waveguides.

Appendix

The components of spectral-domain dyadic Green's function $\tilde{G}$ for the layer structure Fig. 1(c) can be derived by the method

of [25] and [26]. Included here is a typical one such as

$$\tilde{G}_{zz} = \frac{-1}{2\omega\epsilon_0(k_x^2+k_z^2)} \times \left[k_z^2\beta_0\left(e^{-j\beta_0|y-y'|} - \Gamma'_{A0}e^{-j\beta_0(y+y')}\right) + \frac{k_x^2k_0^2}{\beta_0}\left(e^{-j\beta_0|y-y'|} + \Gamma'_{F0}e^{-j\beta_0(y+y')}\right)\right] \quad (11)$$

where

$$\Gamma'_{A0} = (\beta_0 - Z_{A1})/(\beta_0 + Z_{A1}),$$

$$\Gamma'_{F0} = \left(\frac{1}{\beta_0} - Z_{F1}\right)\Big/\left(\frac{1}{\beta_0} + Z_{F1}\right),$$

$$Z_{A1} = \frac{\beta_1}{\epsilon_r(1-j\tan\delta)}\left[\frac{1-\Gamma_{A1}}{1+\Gamma_{A1}}\right],$$

$$Z_{F1} = \frac{1}{\beta_1}\left[\frac{1-\Gamma_{F1}}{1+\Gamma_{F1}}\right],$$

$$\Gamma_{A1} = e^{-2j\beta_1 h}\frac{\frac{\beta_1}{\epsilon_r}\left(\frac{\beta_2}{\epsilon_{r2}} + j\frac{\beta_0}{\epsilon_0}\tan\beta_2 b\right) - \frac{\beta_2}{\epsilon_{r2}}\left(\frac{\beta_0}{\epsilon_0} + j\frac{\beta_2}{\epsilon_{r2}}\tan\beta_2 b\right)}{\frac{\beta_1}{\epsilon_r}\left(\frac{\beta_2}{\epsilon_{r2}} + j\frac{\beta_0}{\epsilon_0}\tan\beta_2 b\right) + \frac{\beta_2}{\epsilon_{r2}}\left(\frac{\beta_0}{\epsilon_0} + j\frac{\beta_2}{\epsilon_{r2}}\tan\beta_2 b\right)},$$

$$\Gamma_{F1} = e^{-2j\beta_1 h}\frac{\frac{1}{\beta_1}\left(\frac{1}{\beta_2} + j\frac{1}{\beta_0}\tan\beta_2 b\right) - \frac{1}{\beta_2}\left(\frac{1}{\beta_0} + j\frac{1}{\beta_2}\tan\beta_2 b\right)}{\frac{1}{\beta_1}\left(\frac{1}{\beta_2} + j\frac{1}{\beta_0}\tan\beta_2 b\right) + \frac{1}{\beta_2}\left(\frac{1}{\beta_0} + j\frac{1}{\beta_2}\tan\beta_2 b\right)}$$

and $\beta_i^2 = k_i^2 - k_x^2 - k_z^2$ $(i = 0,1,2)$, $k_0^2 = \omega^2\epsilon_0\mu_0$, $k_1^2 = \omega^2\epsilon_0\mu_0\epsilon_r(1-j\tan\delta)$, $k_2^2 = -j\omega\sigma$. It should be emphasized again that the superconducting ground plane is now regarded as a lossy layer of wave number k_2, conductivity σ, and thickness b therefore the effect of lossy ground may be discussed by this Green's function.

REFERENCES

[1] A. A. Valenzuela and P. Russer, "High Q coplanar transmission line resonator of $YBa_2Cu_3O_{7-x}$ on MgO," *Appl. Phys. Lett.*, vol. 55, no. 10, pp. 1029–1031, Sept. 1989.

[2] J. H. Takemoto, C. M. Jackson, R. Hu, J. F. Bruch, K. P. Daly, and R. W. Simon, "Microstrip resonators and filters using high-T_c superconducting thin films on $LaAlO_3$," *IEEE Trans. Magn.*, vol. 27, no. 2, pp. 2549–2532, Mar. 1991.

[3] G. C. Liang, R. S. Withers, B. F. Cole, and N. Newman, "High-temperature superconductive devices on sapphire," *IEEE Trans. Microwave Theory Tech.*, vol. 42, no. 1, pp. 34–40, Jan. 1994.

[4] G. C. Liang, R. S. Withers, B. F. Cole, S. M. Garrison, M. E. Johansson, W. S. Ruby, and W. G. Lyons, "High-temperature superconducting delay lines and filters on sapphire and thinned $LaAlO_3$ substrates," *IEEE Trans. Appl. Superconduct.*, vol. 3, no. 3, pp. 3037–3042, Sept. 1993.

[5] R. Ramisch, G. R. Olbrich, and P. Russer, "A tapped-delay-line superconductive chirp filter in shielded microstrip," *IEEE Trans. Microwave Theory Tech.*, vol. 39, no. 9, pp. 1575–1581, Sept. 1991.

[6] W. Chew, A. L. Riley, D. L. Rascoe, B. D. Hunt, M. C. Foote, T. W. Cooley, and L. J. Bajuk, "Design and performance of a high-T_c superconductor coplanar waveguide filter," *IEEE Trans. Microwave Theory Tech.*, vol. 39, no. 9, pp. 1455–1461, Sept. 1991.

[7] G. L. Matthaei and G. L. Hey-Shipton, "Novel staggered resonator array superconducting 2.3-GHz bandpass filter," *IEEE Trans. Microwave Theory Tech.*, vol. 41, no. 12, pp. 2345–2352, Dec. 1993.

[8] J. C. Swihart, "Field solution for a thin-film superconducting strip transmission line," *J. Appl. Phys.*, vol. 32, pp. 461–469, Mar. 1961.

[9] H.-Y. Lee and T. Itoh, "Phenomenological loss equivalence method for planar quasi-TEM transmission lines with a thin normal conductor or superconductor," *IEEE Trans. Microwave Theory Tech.*, vol. 37, no. 12, pp. 1904–1909, Dec. 1989.

[10] D. Nghiem, J. T. Williams, and D. R. Jackson, "A general analysis of propagation along multiple-layer superconducting stripline and microstrip transmission lines," *IEEE Trans. Microwave Theory Tech.*, vol. 39, no. 9, pp. 1553–1565, Sept. 1991.

[11] D. M. Sheen, S. M. Ali, D. E. Oates, R. S. Withers, and J. A. Kong, "Current distribution, resistance and inductance for superconducting strip transmission lines," *IEEE Trans. Appl. Superconduct.*, vol. 1, no. 2, pp. 108–115, June 1991.

[12] S. M. El-Ghazaly, R. B. Hammond, and T. Itoh, "Analysis of superconducting microwave structures: Application to microstrip lines," *IEEE Trans. Microwave Theory Tech.*, vol. 40, no. 3, pp. 499–508, Mar. 1992.

[13] J. Kessler, R. Dill, and P. Russer, "Field theory investigation of high-T_c superconducting coplanar waveguide transmission lines and resonators," *IEEE Trans. Microwave Theory Tech.*, vol. 39, no. 9, pp. 1566–1574, Sept. 1991.

[14] J. M. Pond, C. M. Krowne, and W. L. Carter, "On the application of complex resistive boundary conditions to model transmission lines consisting of very thin superconductors," *IEEE Trans. Microwave Theory Tech.*, vol. 37, no. 1, pp. 181–190, Jan. 1989.

[15] Z. Cai and J. Bornemann, "Generalized spectral-domain analysis for multilayered complex media and high-T_c superconductor applications," *IEEE Trans. Microwave Theory Tech.*, vol. 40, no. 12, pp. 2251–2257, Dec. 1992.

[16] T. E. Van Deventer, P. B. Katehi, J. Y. Josefowicz, and D. B. Rensch, "High frequency characterization of high-temperature superconducting thin film lines," in *1990 IEEE MTT-S Int. Microwave Symp. Dig.*, Dallas, pp. 285–288.

[17] W. Schroeder and I. Wolff, "A hybrid-mode boundary integral equation method for normal- and superconducting transmission lines of arbitrary cross-section," *Int. J. Microwave and Millimeter-Wave Computer-Aided Engineering*, vol. 2, no. 4, pp. 314–330, Oct. 1992.

[18] L. H. Lee, S. M. Ali, and W. G. Lyons, "Full-wave characterization of high-T_c superconducting transmission lines," *IEEE Trans. Appl. Superconduct.*, vol. 2, no. 2, pp. 49–57, June 1992.

[19] L. H. Lee, W. G. Lyons, T. P. Orlando, S. M. Ali and R. S. Withers, "Full-wave analysis of superconducting microstrip lines on anisotropic substrates using equivalent surface impedance approach," *IEEE Trans. Microwave Theory Tech.*, vol. 41, no. 12, pp. 2359–2367, Dec. 1993.

[20] J. Y. Ke and C. H. Chen, "A new approach to the microstrip lines with finite strip thickness and conductivity," in *1993 IEEE MTT-S Int. Microwave Symp. Dig.*, Atlanta, pp. 931–934.

[21] T. P. Orlando and K. A. Delin, *Foundations of Applied Superconductivity*. New York: Addison-Wesley, 1991.

[22] L. H. Lee, S. M. Ali, W. G. Lyons, D. E. Oates, and J. D. Goettee, "Analysis of superconducting transmission line structures for passive microwave device applications," *IEEE Trans. Appl. Superconduct.*, vol. 3, no. 1, pp. 2782–2787, Mar. 1993.

[23] F. Alessandri, G. Baini, G. D'Inzeo and R. Sorrentino, "Conductor loss computation in multiconductor MIC's by transverse resonance technique and modified perturbational method," *IEEE Trans. Microwave Guided Wave Lett.*, vol. 2, no. 6, pp. 250–252, June 1992.

[24] R. Faraji-Dana and Y. L. Chow, "The current distribution and AC resistance of microstrip structure," *IEEE Trans. Microwave Theory Tech.*, vol. 38, no. 9, pp. 1268–1277, Sept. 1990.

[25] T. Itoh, *Numerical Techniques for Microwave and Millimeter-Wave Passive Structures*. New York: Wiley, 1989.

[26] N. K. Dasand and D. M. Pozar, "A generalized spectral-domain Green's function for multilayer dielectric substrates with application to multilayer transmission lines," *IEEE Trans. Microwave Theory Tech.*, vol. 35, no. 3, pp. 326–335, Mar. 1987.

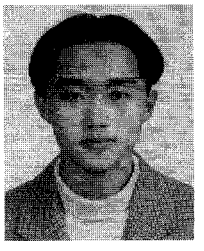

Shau-Gang Mao was born in Kaohsiung, Taiwan, Republic of China, on October 11, 1970. He received the B.S. degree in atmosphere science and the M.S.E.E. degree from National Taiwan University, Taipei, Taiwan, in 1992 and 1994, respectively. Currently, he is pursuing the Ph.D. degree in Electrical Engineering at National Taiwan University.

His research interests include the design and analysis of uniplanar microwave active and passive components.

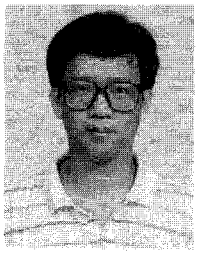

Jeng-Yi Ke was born in Taoyuan, Taiwan, Republic of China, on January 2, 1966. He received the B.S. degree in physics from National Taiwan Normal University, Taipei, Taiwan in 1989, the M.S.E.E. and Ph.D. degrees from National Taiwan University, Taipei, Taiwan in 1991 and 1995, respectively.

His current research interests include analysis of planar transmission lines and leaky wave.

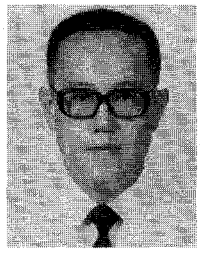

Chun Hsiung Chen was born in Taipei, Taiwan, Republic of China, on March 7, 1937. He received the B.S.E.E. degree from National Taiwan University, Taipei, Taiwan in 1960, the M.S.E.E. degree from National Chiao Tung University, Hsinchu, Taiwan, in 1962, and the Ph.D. degree in Electrical Engineering from National Taiwan University in 1972.

In 1963, he joined the faculty of the Department of Electrical Engineering, National Taiwan University, where he is now a Professor. From 1982 to 1985 he was Chairman of the Department. In 1974 he was a Visiting Researcher for one year in the Department of Electrical Engineering and Computer Sciences, University of California, Berkeley. From 1986 to 1987, he was a Visiting Professor in the Department of Electrical Engineering, University of Houston, Texas. In 1989 and 1990, he visited the Microwave Department, Technical University of Munich, Germany and Laboratoire d'Optique Electromagnetique, Faculte des Sciences et Techniques de Saint-Jerome, Universite d'Aix-Marseille III, France, respectively. His areas of interest include antenna and waveguide analysis, propagation and scattering of waves, and numerical techniques in electromagnetics.